Molecular dynamics study of free energy profile for dissociation of ligand from CA I active site

MS Arwansyah*[1,2], Koichi Kodama[1], Isman Kurniawan[1,3], Tatsuki Kataoka[1], Kazutomo Kawaguchi[1], and Hidemi Nagao[1]

[1]Division of Mathematical and Physical Sciences, Graduate School of Natural Science and Technology, Kanazawa University, Kanazawa 920-1192, Japan
[2]School of Chemistry, University of Cokroaminoto Palopo, Palopo, Indonesia
[3]School of Computing, Telkom University, Jl. Telekomunikasi, Terusan Buah Batu, Bandung, Indonesia

Abstract   We investigate the binding/dissociation process of ligand molecule from carbonic anhydrase (CA) I carbonic anhydrase (CA) I enzyme by using all-atom molecular dynamics simulation. The force field parameters of zinc ion in the CA I active site are estimated by quantum chemical calculations and are summarized in this paper. The free energy profile for binding/dissociation process of ligand from CA I active site is calculated by the thermodynamic integration combined with the all-atom molecular dynamics simulation. The binding free energy as a function of the distance between the center of mass positions of CA I active site and the ligand molecule is estimated. The radial distribution function of the CA I-ligand complex is calculated from the trajectory of all-atom molecular dynamics (MD) simulation. We estimate the free energy surface from the radial distribution function. We can obtain the bond constant of the equilibrium state from the value of the free energy surface. We discuss the binding/dissociation process of ligand molecule by calculating the free energy profile to know the stability of the CA I-ligand complex with some thermodynamic properties such as the binding free energy, the equilibrium state of the free energy surface and so on.

Keywords.   CA I active site, ligand molecule, force field parameters, free energy profile, free energy surface.

1   Introduction

Carbonic anhydrases (CAs) family is a ubiquitous zinc enzyme which can be isolated from archaea, prokaryotes, and eukaryotes [1]. In higher vertebrates including human, 14 different CA isozymes are found in several subcellular localizations such as CAI-III and CA VII found in cytosols, CA IV, CA IX, CA XII, and CA XIV located in membrane, CA V found in mitochondria, and CA VI secreted in saliva [1, 2]. These enzymes involve the biological fundamental roles such as catalyzes of the hydration of carbon dioxide to bicarbonate which is essential to regulate the pH levels in cells, biosynthetic reaction and electrolyte secretion in several tissues [1–4].

Corresponding author   Email: arwan@wriron1.s.kanazawa-u.ac.jp.

The structures of carbonic anhydrases have been investigated by X-ray analysis [5–9]. All isozymes of carbonic anhydrase contain a zinc ion in the enzyme active site which is essential for catalytic activity. Three histidine residues coordinate to Zn ion through their imidazole nitrogen atoms. A water molecule occupies the fourth coordinated position in the active site at an acidic pH (< 7) or a hydroxyl ion at higher pH with tetrahedral coordination geometry through proton-transfer reaction from water binding to the zinc ion in the CAs active site [10, 11]. The selected inhibitor can be applied to change the position of the water molecule or hydroxyl group to inhibit the biological process in cells. The sulfonamide group of a heterocyclic structure can also be applied in the primary application as the most potent inhibitors that bind to the zinc ion through the deprotonated nitrogen. The sulfonamide group is implemented to have an anticonvulsant, antiglaucoma, anticancer, and antiurolithic [4].

Almost every CAs family relates to some diseases such as glaucoma, diabetes, cancer, epilepsy, and etc [12, 13]. The several ligand molecules to inhibit CAs activity are the critical target for the therapeutics against many diseases. Therefore, understanding the interaction between ligand and CAs including Zn ion is crucial. The several computational studies on CAs have been recently performed [14–16]. The interaction of some antiepileptic drugs with CA active center has been quantum mechanically investigated to elucidate the relative orientations of CA II-inhibitor complex using a high-level calculation to understanding on the mechanism of inhibitor action [14]. All-atom molecular dynamics (MD) simulation of CA enzyme has also been carried out for CA II enzyme in complex with ligand (acetazolamide) to obtain a theoretical understanding of metalloprotein-inhibitor complex [15]. This paper shows the quantitative insight into the binding interaction of protein-ligand complex and represents the key role in Zn ion in the CAs active site. The theoretical studies on the standard free energy of protein-ligand binding have been investigated to understand the free energy change of the ligand molecules in the binding/dissociation process [15–19].

In this paper, we investigate the binding free energy between CA I enzyme and the ligand molecule. The force field parameters of the zinc ion in the CA I active site is estimated by quantum chemical calculations. The free energy profile for binding/dissociation process of ligand from CA I active site is calculated by using thermodynamic integration combined with all-atom MD simulation according to the procedure provided in the previous work [20, 21]. We discuss the binding/dissociation process of ligand molecule by calculating the free energy profile to know the stability of CA I-ligand complex related to some thermodynamic properties such as the binding free energy, the equilibrium state of the free energy surface and so on.

2   Method and model

In this section, we present a model using in this simulation conditions for MD simulation. The force field parameters in the CA I active site are estimated, and the free energy profile is introduced. The free energy profile as a function of the distance between the center of mass positions of CA I active site and the ligand molecule, r_{cm}, is calculated by all-atom MD simulation with the thermodynamic integration method presented in the previous work [19, 22].

2.1   Model for molecular dynamics simulation

In this study, the structure of CA I in complex with the ligand molecule (4-carboxyethyl benzene-sulfonamide ethyl ester) is obtained from the X-ray crystallographic structure in the protein data bank solved by Srivastava, *et al.* (PDB ID: 2NN7) and is applied to initial structure for the simulation of ligand binding/dissociation process [23]. In the CA I enzyme, the total number of residues
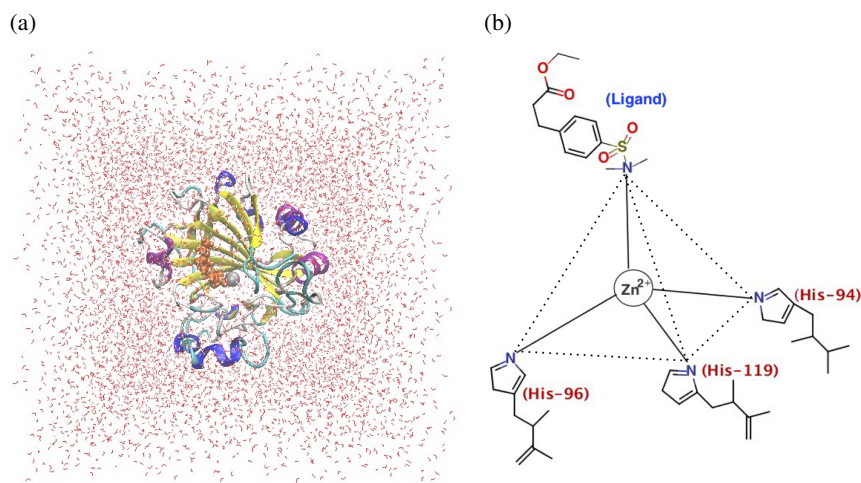
(a)   (b)

Figure 1: (a) The structure of CA I in complex with the ligand, Zn^{2+}, and water molecules are placed into a cubic box. CA I is represented by cartoon model. Ligand and Zn^{2+} ion are represented by VDW model and silver spheres, respectively. (b) The cluster model of CA I active site in Zn^{2+} ion which is tetrahedrally coordinated with three histidine residues (His 94, 96, 119) and ligand molecule.

is 260 which consists of a zinc ion, 10 helices and 18 strands of the beta sheet with the total number of atoms being 2029. The ligand is a derivative of benzenesulfonamide CA inhibitor which contains 17 atoms. The structure of CA I enzyme and ligand immersed by water molecules are shown in Fig. 1(a).

2.2   Force field parameters in metal

The cluster model of CA I active site consists of a zinc ion and three histidine residues (His 94, 96, 119) which are tetrahedrally coordinated with a ligand molecule as shown in Fig. 1(b). The CA I active site in complex with ligand is calculated by the quantum chemical methods to know the interaction effect of the stability from the interaction of zinc ion with histidine residues and ligand molecule.

The force field parameters of zinc ion in the CA I active site are not available in the Zinc AMBER force field (ZAFF) database developed by Peters *et al* [24]. Therefore, we evaluate the force field parameters of zinc ion in the CA I active site by calculating the potential energy surface (PES) as a function of bond distance and bond angle. The bond distance and angle potential are provided as follows:

$$V(r, K_r) = K_r(r - r_c)^2, \tag{2.1}$$

$$V(\theta, K_\theta) = K_\theta(\theta - \theta_c)^2, \tag{2.2}$$

where K_r and K_θ are the force constants of distance and angle respectively, and r_c and θ_c are equilibrium distance and angle, respectively. The structure of CA I is optimized by freezing the heavy atoms. The potential energy surface of bond distance and bond angle of CA I is analyzed by using the B3LYP method with the 6-31G* basis set with the increment of 0.02 and $2°$, respectively. The range of increment is determined to avoid the inharmonic effect of distance and angle according to the suggestion in Ref. [25, 26]. The optimized structure and potential energy surface calculations for distance and angle are performed by Gaussian 09 packages [27]. Then, we convert the quantum chemical calculation of the distance and angle of zinc-N(His 94, 96, 119) motif in the CA I active site into the Amber force field parameters by using Metal Center Parameter Builder (MCPB) [28]. Our force field parameters have not been submitted to the AMBER parameter database.

2.3   Simulation condition

All-atom molecular dynamics simulation is performed on CA I enzyme and ligand molecule. The TIP3P water model [29] with 9808 water molecules inserted in a $70 \times 69 \times 77$ Å^3 periodic box then, 3 Cl$^-$ ions are added to neutralize the whole system. The total number of atoms in the system is 33,425. The AMBER14 force field is used for the protein molecule [30], and general AMBER force field (GAFF) is applied to determine the force field parameters of ligand molecule. The electrostatic interactions are computed by using the Particle Mesh Ewald (PME) algorithm. The switching cutoff distance is 10 Å. The SHAKE algorithm is used to constrain the bond distance of the hydrogen atoms. A time step of 2 fs is applied in all simulations.

The energy minimization of the system is carried out with the constraint on the position of the heavy atoms of CA I, ligand and Cl$^-$ ion. Then, we perform the energy minimization without any constraint. The system is simulated on NVT-constant simulation for 60 ps where the temperature is gradually increased from 0 to 300 K. The temperature and pressure of the system are kept at 300 K and 1 atm by using the Langevin thermostat and isotropic position scaling algorithm, respectively. We equilibrate the system with the NPT ensemble for 50 ns without the harmonic positional constraint. After the whole system reaches the equilibrium state, the production run with a constraint on the distance between the centers of mass of CA I active site and the ligand is performed. The SHAKE method is used to constraint the distance. We prepared 19 distances with the increment of 0.5 Å: r= 6-15 Å. Each simulation is performed for 5 ns with NPT-constant MD simulation to obtain the mean force $< F(r') >$ from the MD trajectory. All MD simulations are carried out by Amber 16 packages [30]. The analysis of the trajectories of MD simulation is performed by CPPTRAJ tools [31].

2.4   Root-mean-square deviation

We calculate the root-mean-square deviation (RMSD) of Cα atoms of CA I enzyme and the heavy elements of ligand molecule according to the following equation:

$$RMSD(t_1) = \left[\frac{1}{M} \sum_{i=1}^{N} m_i \parallel r_i(t_1) - r_{ref,i} \parallel^2 \right]^{\frac{1}{2}}, \tag{2.3}$$

where m_i is the mass of atom i, N is the total number of Cα atoms of CA I enzyme and the heavy elements of ligand, M is the total mass of Cα atoms in CA I and the heavy elements of ligand molecule, $r_i(t)$ is the position of the Cα atom of protein and C, N, O, and S atoms of ligand at the time t, and $r_{ref,i}$ is the position of ith atom in the X-ray structure.

2.5   Free energy calculation

We calculate the ligand dissociation process from the CA I active site by generating the free energy profile $\Delta G(r)$ as a function of the distance, r_{cm}, between the centers of mass of ligand and CA I active site as follows [32, 33]:

$$\Delta G(r) = G(r) - G(r_0)$$
$$= \int_{r_0}^{r} \left(\frac{dG(r')}{dr'} \right) dr' \tag{2.4}$$
$$= \int_{r_0}^{r} < \frac{\partial U}{\partial r'} >_{r'} dr,'$$

where U is the potential energy of the whole system, r_0 is a reference distance, $G(r)$ is the free energy of the whole system, and $< ... >'_r$ represents the isothermal-isobaric ensemble average, where the distance r_{cm} is constrained to r'. The free energy profile is evaluated by [33–35] as follows :

$$\Delta G(r) = - \int_{r0}^{r} < F(r') >_{r'} dr',$$

$$F(r') = \left(\frac{m_{pro}}{m_{pro} + m_{lig}} \boldsymbol{F}_{lig} - \frac{m_{lig}}{m_{pro} + m_{lig}} \boldsymbol{F}_{pro} \right) \cdot \boldsymbol{n}, \qquad (2.5)$$

where $F(r')$ is the mean force at r_{cm}, $\boldsymbol{F}_{lig}$ and $\boldsymbol{F}_{pro}$ are forces at r_{cm}, m_{pro} and m_{lig} are the total masses of the CA I active site and ligand, respectively, and $\boldsymbol{n}$ is the unit vector from the center of mass of the CA I active site to that of the ligand molecule. Then, $\Delta G(r)$ can be calculated by [20, 36] as follows:

$$\Delta G(r) \cong - \sum_{i=1}^{Nw} \frac{1}{2} (< F(r') >_{r'=r_i} + < F(r') >_{r'=r_{i-1}})(r_i - r_{i-1}). \qquad (2.6)$$

The free energy profile of the ligand dissociation as a function of the distance between the centers of mass of the CA I active site and the ligand molecule can be calculated using $< F(r') >$ from trajectories of MD simulations.

3   Results and Discussion

In order to investigate the dissociation process of the ligand molecule from the CA I active site, we estimate the thermodynamic properties of ligand binding/dissociation which can be obtained from the free energy profile as a function of r_{cm}. In this section, we determine the force field parameters of the zinc ion in the CA I active site for MD simulation and then estimate the free energy profile of the ligand molecule in the binding/dissociation process by the thermodynamic integration method. Finally, we discuss the dynamic of the complex in equilibrium state related to the free energy surface estimated from the radial distribution function.

3.1   Force field parameters

The structure of model cluster as shown in Fig. 2 in CA I active is optimized to obtain a good relative spatial arrangement of its structure. The residues (His 94, 96, 119) of CA I active site in complex with ligand are connected to the Zn center represented by the tetrahedral coordination structure. The schematic diagram of the charge distribution of the CA I active site is also shown in Fig. 3.

The potential energy surfaces (PES) of bond and of angle of CA I active site are shown in Fig. 4. The equilibrium bond distances of Zn-N(His94), Zn-N(His96) and Zn-N(His119) are around 1.999, 2.024 and 2.018 Å respectively as shown in Fig. 4(a). The fitted force constant (Kq) for Zn-N(His94), Zn-N(His96), and Zn-N(His119) is 93.419, 96.543, and 96.135 kcal mol^{-1} Å^{-2}, respectively. The PES of the equilibrium angle of X-Zn-Y (X,Y) = (N(His94), N(His96)), (N(His94), N(His119)), (N(His96), N(His119)) was 108.531°, 112.021°, 108.172°, respectively (Fig. 4(b)). The fitted force constant (Kq) for (His94)N-Zn-N(His96), (His96)N-Zn-N(His119), and (His94)N-Zn-N(His119) is 72.351, 77.055, and 71.863 kcal mol^{-1} rad^{-2}, respectively. Table 1 summarizes the bond and angle parameters of zinc ion in the CA I active site from the
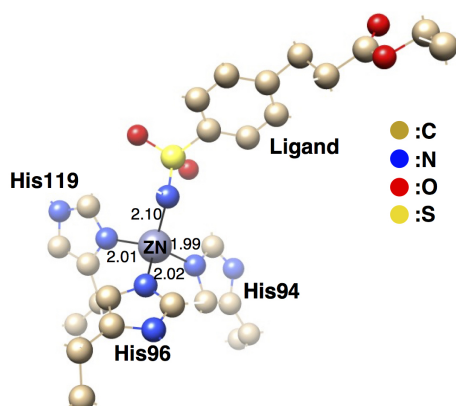
Figure 2: The optimized structure of CA I active site in complex with ligand molecule in which the zinc ion is located at the center of a deep, silver spheres model, tetrahedrally coordinated with three histidine residues (His 94, 96, 119) and ligand molecule.
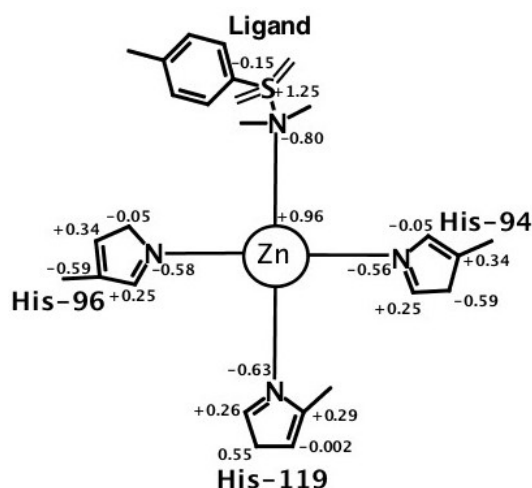

Figure 3: Charge distribution around the CA I active site.

experimental values and quantum chemical calculations. The experimental values of bond and angle parameters are estimated from the mean values (with standard deviations) of the eight X-ray crystallographic structures of CA I sharing the Zinc-N(His 94, 96, 119) motif. From Table 1, we find that the values of the equilibrium distances for Zn-N(His94), Zn-N(His96) and Zn-N(His119) calculated by quantum chemical method was similar to those obtained by the experimental results, and the angle of (His94)N-Zn-N(His96) is the most favorable parameter with similar values of the experimental results. The bond and angle force field parameters of zinc ion in the CA I active site are evaluated by quantum chemical calculation according to the calculation procedure in Ref. [37] and [38].

3.2   Molecular dynamics simulation

The root-mean-square deviation (RMSD) value defined in Equation (2.3) is evaluated to check the stability of the CA I in complex with the ligand molecule from the initial modeling structure by X-ray analysis. Fig. 5(a) shows the time evolution of the RMSD value which is obtained from the MD simulation of the CA I in complex with the ligand, and the simulated system almost becomes the equilibrium state at 2 ns. From Fig. 5(b), we find that the average distance of r_{cm}
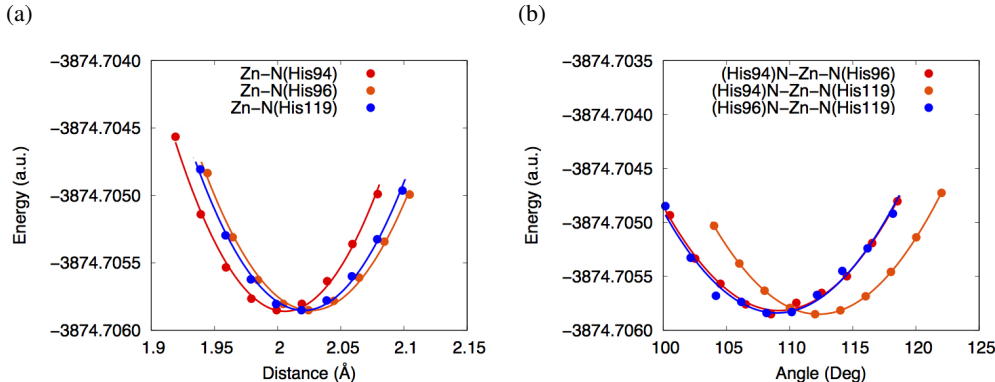
(a) (b)

Figure 4: The potential energy surface (PES) (a) PES for bond distance between Zn and X (X=N(His94, His96, His94)), (b) PES for bond angle X-Zn-Y ((X,Y)= (N(His94), N(His96)), (N(His94), N(His119)), (N(His96), N(His119))

Table 1: Bond and angle parameters of zinc ion in the CA I active site. The standard deviations are shown in parentheses.

Bond Distance	$r_{\text{experiment}}$[a] (Å)	r_{QC} (Å)	K_q (kcal mol^{-1} Å^{-2})
Zn-N(His94)	2.040 (0.051)	1.999	93.419
Zn-N(His96)	2.125 (0.083)	2.024	96.543
Zn-N(His119)	2.063 (0.054)	2.018	96.135
Bond Angle	$\theta_{\text{experiment}}$[a] (°)	θ_{QC} (°)	$K\theta$ (kcal mol^{-1} rad^{-2})
(His94)N-Zn-N(His96)	107.175 (2.539)	108.531	72.351
(His94)N-Zn-N(His119)	110.958 (4.859)	112.021	77.055
(His96)N-Zn-N(His119)	102.174 (5.296)	108.172	71.863
Zn-N(His94)-Cβ	121.166 (4.450)	126.848	198.938
Zn-N(His94)-Cγ	130.514 (5.240)	126.571	198.838
Zn-N(His96)-Cβ	138.397 (6.745)	128.203	204.398
Zn-N(His96)-Cγ	112.348 (6.839)	125.474	96.542
Zn-N(His119)-Cβ	131.993 (2.190)	127.997	201.740
Zn-N(His119)-Cγ	117.769 (1.975)	124.874	191.955

[a] The experimental data obtained from the X-ray crystallographic structures of CA I sharing the Zinc-N(His 94, 96, 119) motif in the protein data bank (PDB ID: 2NN7 [23], 2NN1 [23], 2NMX [23], 1AZM [39], 1BZM [39], 3LXE [40], 4WUQ [41], 6EVR [42].)

for the last 3.0 ns is 8.58 Å with the standard deviation of 0.29 Å. Fig. 6 shows the fluctuation of the distances and angles in the CA I active site. We obtain that the distances of zinc-N(His 94, 96, 119) motif are 1.95± 0.05, 2.00± 0.05, and 2.01± 0.06 Å and the angles of X-Zn-Y ((X,Y)= (N(His94), N(His96)), (N(His94), N(His119)), (N(His96), N(His119)) are 107.73± 3.14, 113.64± 2.76, 103.40± 2.94, respectively. These results are consistent with those of the distances and angles from quantum chemical calculation in Table 1. We assume that the distances and angles of zinc-N(His 94, 96, 119) motif in the CA I active site become stable during the 50 ns simulation.
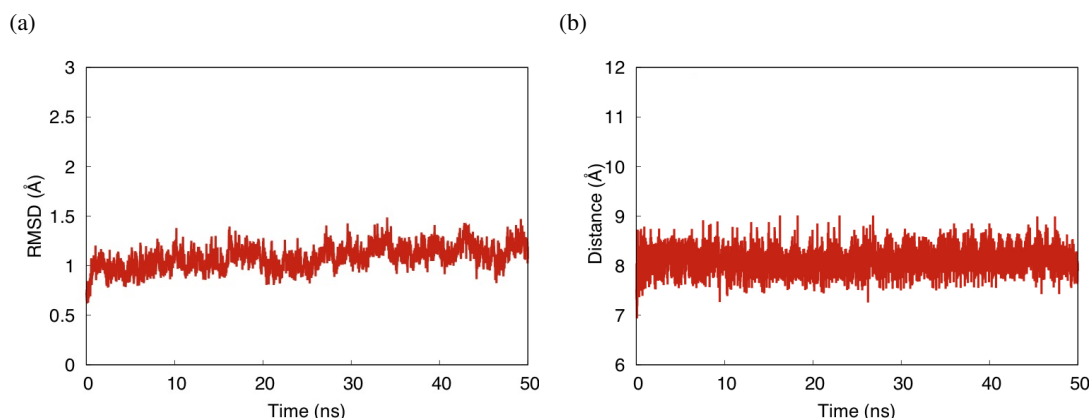
(a)

(b)

Figure 5: (a) The RMSD value of CA I-Ligand complex, (b) the distance between the center of mass of ligand and that of CA I active site during the simulation.
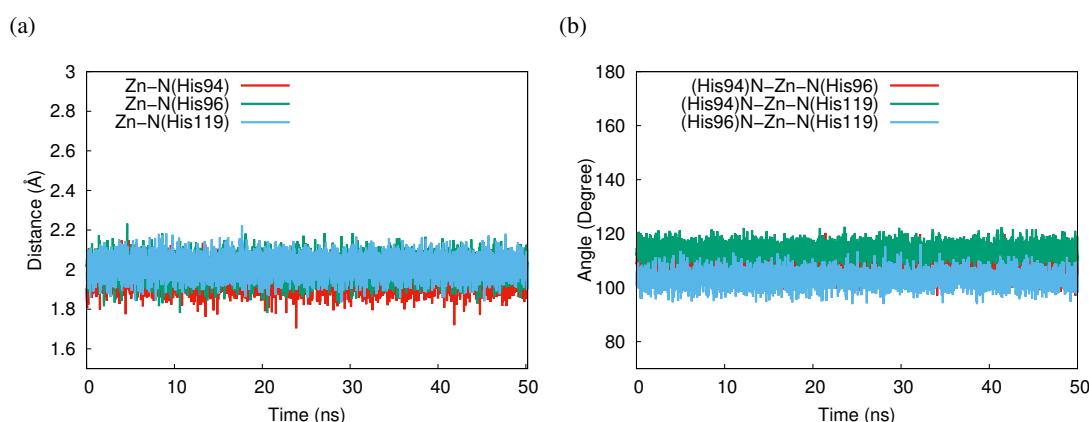
(a)

(b)

Figure 6: (a) The distance and (b) angle fluctuation in the CA I active site during the simulation.

3.3   Free energy profile

The mean force $< F(r') >$ derived in Equation (2.5) is estimated at each r_{cm} values shown in Fig. 7(a). The error bars represent the standard deviation which is obtained from the independent measurements of $< F(r') >$ for each 5-ns trajectory of MD simulation. The repulsive force between CA I active site and ligand is represented as the positive value of $< F(r') >$, while the negative value represents an attractive force between CA I active site and ligand. The attractive force between CA I active site and ligand molecule is observed at the distance of 9 Å $\leq r_{cm} \leq$ 15 Å, while the repulsive force at the distance of 6 Å r_{cm} 8.5 Å. We assume that the distance of 15 Å is the reference state, because the mean force at the position becomes small at around 5.4×10^{-11}N. It implies that the interaction between CA I and ligand molecule almost vanishes at the reference state. We observe that the error bar at r_{cm} 14.5 Å is smaller than the other distances, and it suggests that the conformational change of ligand molecule has small fluctuation around the side chains of CA I active site and, on the other hand, that the error bar at r_{cm} 11 Å has large value because of the large fluctuation of the ligand conformation in the side chains of CA I active site.

Fig. 7(b) shows the free energy profile as a function of r_{cm} derived in Equation (2.6). Here, we discuss the binding free energy from the reference state (r_{cm}= 15 Å) and not from the standard state of the binding free energy. The binding free energy from the reference state is calculated by using thermodynamic integration method to elucidate the stabilization of the ligand molecule in the binding pocket of CA I enzyme. The binding free energy as shown in Ref. [43] has been calculated
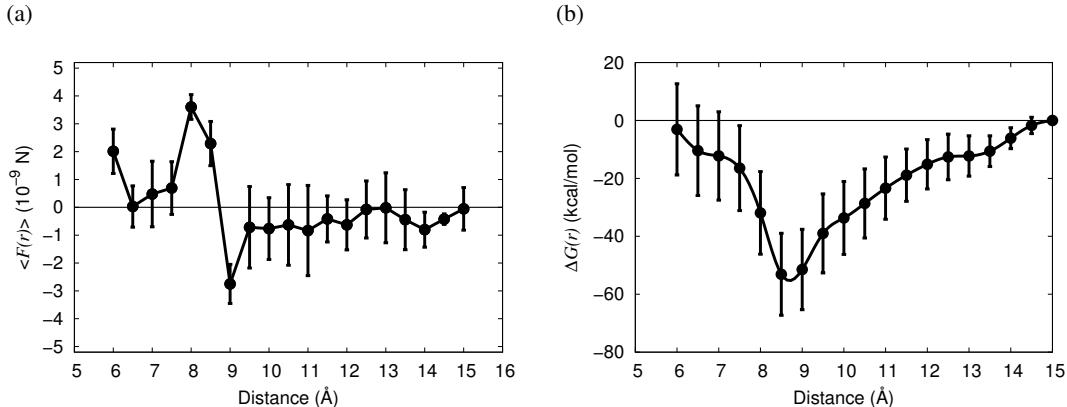
(a)   (b)

Figure 7: (a) The mean force $< F(r') >$ and (b) free energy profile $G(r)$ as a function of the distance between the center of mass of ligand and that of CA I active site. The error bars represent the standard deviation for all the trajectories of MD simulation

by a method to calculate the binding free energy with reference to the standard state. The standard chemical potential of each molecule is defined as a hypothetical standard state where the molecule in the system occupies at standard concentration in the reaction solvent. From Fig. 5(b), we can approximately estimate the binding free energy of the complex from the reference state of -53.11$\pm$ 14.17 kcal/mol and the free energy reaches the minimum at r_{cm} 8.5 Å. This result is consistent with that of the equilibrium MD, in which the average value is r_{cm} 8.58 Å. Meanwhile, the calculated binding free energy (-53.11 kcal/mol) is underestimated compared to Ref. [15]. However, for the case of the binding free energy of protein/ligand complex, the energy could be around -53.11 kcal/mol or more [19, 44, 45]. Unfortunately, we cannot validate at present the estimated binding free energy because there is no corresponding experimental result available for the binding free energy along the distance between CA I/ ligand complex. However, we believe that our results contribute to giving an insight for estimation of the free energy profile as the function of the binding distance.

3.4   Free energy surface around the binding state

In the previous subsection, we have estimated the free energy profile corresponding to the binding/dissociation process between the CA I active site and the ligand as shown in Fig. 7(b) and have estimated the binding free energy between the molecules. However, the standard deviation of free energy is not so small at the equilibrium state. Therefore, it is not easy to know the detail of behavior of the dynamics of CA I and ligand complex at the equilibrium state of the association from Fig. 7(b). For the purpose, we try to investigate the dynamics of the complex from the viewpoint of another physical approach.

Fig. 8 shows the radial distribution function (RDF) as a function of r_{cm}. The radial distribution function (RDF) $g(r_{cm})$ can be calculated from the trajectory of all-atom MD simulation for the last 3 ns. The value of the first peak is represented as $g(r_{cm}) = \rho(r_{cm})/\rho_{max}$, where $\rho(r_{cm})$ and ρ_{max} represent the number of density at the distance r_{cm} and the highest peak value, respectively. We find that the position of the peak of the radial distribution function is 8.58 Å. The value of r_{cm} in the X-ray analysis is 8.58 Å. This result is the similar value obtained from RDF calculation as shown in Fig. 8. The free energy surface can be estimated as $G(r_{cm}) = k_B T \ln g(r_{cm})$, where k_B, T, and $g(r_{cm})$ correspond to the Boltzmann constant, temperature and the radial distribution function for the distance between the centers of mass of CA I active site and ligand molecule, respectively.
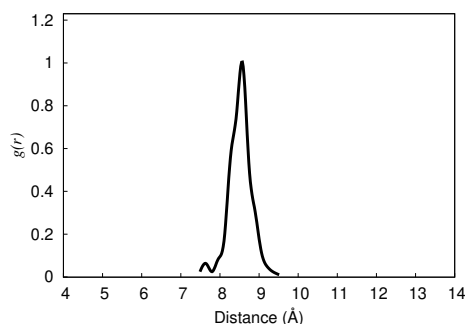
Figure 8: The radial distribution function (RDF) of the distance between the center of mass of ligand and that of CA I active site.
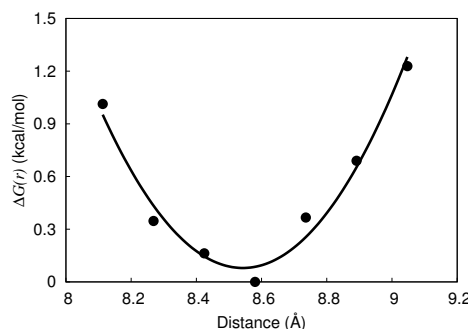

Figure 9: The free energy profile obtained from RDF data in Figure 6.

Fig. 9 shows the free energy surface obtained from the radial distribution function, where the value of the free energy is calculated from the equilibrium state, and the horizontal axis represents the distance between the center of mass of CA I active site and that of ligand molecule. The lowest free energy value along the distance is observed at the distance of 8.58 Å and we can find that the minimum distance is similar to that obtained by thermodynamic integration calculations. From Fig. 9, we can find the harmonicity of the free energy around the equilibrium state and can estimate the bond constant from the equilibrium state of the free energy surface as 271.72 kcal mol^{-1} Å^{-2} at the distance of 8.58 Å. The bond potential is represented as $F(r_{cm}) = K(r_{cm} - r_0)^2$, where K and r_0 are the bond constant and equilibrium distance, respectively.

3.5   Binding Free Energy based on MM/PBSA calculation

The binding free energy between CA I and ligand from the reference state has been calculated in the previous subsection. We have also calculated the radial distribution function as a function of r_{cm}. The free energy surface around the equilibrium state has been determined from the RDF value. However, we can not obtain the binding free energy from the standard state. Therefore, we investigate the binding free energy of the protein-ligand complex in water solvent by estimating the gas-phase interaction energy E_{MM}, solvation free energy E_{Solv}, and entropy $-T\Delta S$ of the complex. These energies represent as $\Delta G_{bind} = \Delta E_{MM} + \Delta G_{Solv^{PBSA}} - T\Delta S$. The gas-phase interaction energy between CA I and ligand is given by $\Delta E_{MM} = \Delta E_{ele} + \Delta E_{vdw}$, where ΔE_{ele} and ΔE_{vdw} are the van der Waals and the electrostatic energies, respectively. The solvation free energy ΔG_{Solv}^{PBSA} is estimated by using continuum approach (Poisson-Boltzmann/surface area), i.e., $G_{Solv^{PBSA}} = G_{Solv^{PB}} + G_{Solv}^{SA}$. The contribution energies as shown in the equation above are calculated by using MM/PBSA program and Normal mode analysis (Nmode) [46] in the Amber 16 packages. All the binding free energies of CA I/ligand complexes are calculated by using a single configuration obtained from the procedure described in the section above (simulation condition).

Table 2 lists the contribution of the molecular mechanics and solvation energies of the CA I enzyme obtained from the several PDB files with some different ligands. From Table 2, we obtain that the binding free energy for all CA I/ligand complexes are good aggrement with the experimental results. For the fourth of the binding free energies, the van der Waals energies are not significantly different, which implies they all have good hydrophobic interactions. However, we find that the electrostatic energies (ΔE_{ele}) are different with values of -119.25, -166.54, -129.35, -130.79 kcal/mol. We conclude that the electrostatic term influences for determining the different binding orientations.

Table 2: The binding free energy and the contribution of each energy term. The standard deviations are shown in parentheses. Units are in kcal/mol.

PDB ID	Total Charge	ΔE_{vdw}	ΔE_{ele}	ΔG_{Solv}^{PB}	ΔG_{Solv}^{SA}	E_{MM}	ΔG_{Solv}^{PBSA}	$-T\Delta S$	G_{bind}^{calc}	G_{bind}^{Exp}
2NN7	-3.00	-16.93	-119.25	89.25	-3.21	-136.18	86.04	-41.50	-8.64	-9.57 [a]
2NN1	-2.00	-10.60	-166.54	130.56	-2.64	-177.14	127.92	-41.90	-7.32	-8.43 [a]
2NMX	-1.00	-14.66	-129.35	97.70	-2.93	-144.01	94.77	-41.72	-7.52	-7.61 [a]
1AZM	-1.00	-11.51	-130.79	103.57	-2.49	-143.87	101.07	-34.72	-8.08	-8.29 [b]

The experimental values for the binding free energy of CA I/ligand complexes are obtained from the Ref. [23][a] and Ref. [39][b].

4   Summary

In this study, we have performed the all-atom MD simulation of the CA I complex with the ligand molecule. We have presented a simple cluster model derived from the structure by X-ray analysis to obtain the force field of the zinc ion in the CA I active site. The force field parameters related to the zinc ion with MD simulation has been summarized. The free energy profile of the binding/dissociation process of ligand from the CA I enzyme has been estimated by some integration methods. We have discussed the free energy surface of the CA I enzyme with the ligand in relation to the radial distribution function of the distance between the centers of mass of CA I enzyme and the ligand molecule.

In the estimation of free energy profile, the mean force acting on between the CA enzyme and the ligand has been estimated at each distance between the center of the molecule from the MD simulation. We have found that the attractive force can be observed at the longer distance than the equilibrium distance and that the repulsive force can be observed in the shorter distance than the equilibrium distance. From the mean force, we have calculated the free energy profile. The results of free energy profile suggest that the equilibrium distance derived from MD simulations is a good agreement with the experimental distance, and we have estimated the binding free energy of -53.11± 14.17 kcal/mol. Meanwhile, we calculate the free energy surface between the CA I enzyme and the ligand by the radial distribution function estimated from the MD trajectories. We have found the harmonicity of the free energy surface around the equilibrium distance between two molecules with the bond constant of 271.72 kcal mol^{-1} Å^{-2} at the equilibrium point at the distance of 8.58 Å.

We have also calculated the binding free energy based on MM/PBSA calculation to estimate the contribution of the molecular mechanics and solvation energies of several CA I/ligand complexes. We observe that the electrostatic energy is the predominant impact for determining the binding free energy of the complexes.

Acknowledgements

References

[1] C. T. Supuran, F. Briganti, S. Tilli, W. Chegwidden, A. Scozzafava, "Carbonic anhydrase inhibitors: sulfonamides as antitumor agents?" Bioorg. Med. Chem 9 (3) (2001) 703–714.

[2] C. T. Supuran, A. Scozzafava, A. Casini, "Carbonic Anhydrase Inhibitors," Med. Res. Rev 23 (2) (2003) 146–189.

[3] C. T. Supuran, A. Scozzafava, "Applications of carbonic anhydrase inhibitors and activators in therapy," Expert Opin. Ther. Pat. 12 (2) (2002) 217–242.

[4] C. T. Supuran, A. Scozzafava, "Carbonic anhydrase inhibitors and their therapeutic potential," Expert Opin. Ther. Pat. 10 (5) (2000) 575–600.

[5] S. K. Nair, J. F. Krebs, D. W. Christianson, C. A. Fierke, "Structural basis of inhibitor affinity to variants of human carbonic anhydrase II," Biochemistry 34 (12) (1995) 3981–3989.

[6] D. A. Whittington, A. Waheed, B. Ulmasov, G. N. Shah, J. H. Grubb, W. S. Sly, D. W. Christianson, "Crystal structure of the dimeric extracellular domain of human carbonic anhydrase xii, a bitopic membrane protein overexpressed in certain cancer tumor cells", Proc. Natl. Acad. Sci. U. S. A. 98 (17) (2001) 9545–9550.

[7] M. Ferraroni, S. Tilli, F. Briganti, W. R. Chegwidden, C. T. Supuran, K. E. Wiebauer, R. E. Tashian, A. Scozzafava, "Crystal structure of a zinc-activated variant of human carbonic anhydrase I, CA I Michigan 1: Evidence for a second zinc binding site involving arginine coordination," Biochemistry 41 (20) (2002) 6237–6244.

[8] J. Leitans, A. Kazaks, A. Balode, J. Ivanova, R. Zalubovskis, C. T. Supuran, K. Tars, "Efficient Expression and Crystallization System of Cancer-Associated Carbonic Anhydrase Isoform IX," J. Med. Chem. 58 (22) (2015) 9004–9009.

[9] P. Řezáčová, D. Borek, S. F. Moy, A. Joachimiak, Z. Otwinowski, "Crystal structure and putative function of small Toprim domain-containing protein from Bacillus stearothermophilus," Proteins: Structure, Function, and Bioinformatics 70 (2) (2008) 311–319. doi:10.1002/prot.21511.

[10] W. S. Sly, P. Y. Hu, "Human carbonic anhydrases and carbonic anhydrase deficiencies," Annu. Rev. Biochem. 64 (1995) 375–401.

[11] S. Pastorekova, S. Parkkila, J. Pastorek, C. T. Supuran, "Carbonic anhydrases: Current state of the art, therapeutic applications and future prospects," J. Enzyme Inhib. Med. Chem. 19 (3) (2004) 199–229.

[12] A. Scozzafava, L. Menabuoni, F. Mincione, F. Briganti, G. Mincione, C. T. Supuran, "Carbonic anhydrase inhibitors. synthesis of water-soluble, topically effective, intraocular pressure-lowering aromatic/heterocyclic sulfonamides containing cationic or anionic moieties: is the tail more important than the ring?," J. Med. Chem. 42 (14) (1999) 2641–2650.

[13] C. T. Supuran, A. Scozzafava, "Carbonic anhydrases as targets for medicinal chemistry," Bioorg. Med. Chem. 15 (13) (2007) 4336–4350.

[14] M. Ghiasi, S. Kamalinahad, M. Arabieh, M. Zahedi, "Carbonic anhydrase inhibitors: A quantum mechanical study of interaction between some antiepileptic drugs with active center of carbonic anhydrase enzyme," Comput. Theor. Chem. 992 (2012) 59–69.

[15] T. O. Wambo, L. Y. Chen, S. F. McHardy, A. T. Tsin, "Molecular dynamics study of human carbonic anhydrase II in complex with Zn2+and acetazolamide on the basis of all-atom force field simulations," Biophys. Chem. 214-215 (2016) 54–60.

[16] Y. Deng, B. Roux, "Computations of Standard Binding Free Energies with Molecular Dynamics Simulations," J. Phys. Chem. B 113 (8) (2009) 2234–2246. doi:10.1021/jp807701h.

[17] S. Doudou, N. A. Burton, R. H. Henchman, "Standard free energy of binding from a one-dimensional potential of mean force," J. Chem. Theory Comput. 5 (4) (2009) 909–918.

[18] I. J. General, "A Note on the Standard State's Binding Free Energy," J. Chem. Theory Comput. 6 (8) (2010) 2520–2524.

[19] K. Kawaguchi, H. Saito, H. Nagao, S. Okazaki, "Molecular dynamics study on the free energy profile for dissociation of adp from n-terminal domain of hsp90," Chem. Phys. Lett. 588 (2013) 226–230.

[20] K. Kawaguchi, H. Saito, H. Nagao, "Decomposition analysis of free energy profile for Hsp90-ADP association," Mol. Simul. 42 (11) (2016) 896–901.

[21] S. Nakagawa, I. Kurniawan, K. Kodama, M. S. Arwansyah, K. Kawaguchi, H. Nagao, "Theoretical study on interaction of cytochrome f and plastocyanin complex by a simple coarse-grained model with molecular crowding effect," Mol. Phys. 116 (5-6) (2018) 666–677.

[22] K. Kawaguchi, S. Nakagawa, S. Kinoshita, M. Wada, H. Saito, H. Nagao, "A simple coarse-grained model for interacting protein complex," Molecular Physics 115 (5) (2017) 587–597.

[23] D. K. Srivastava, K. M. Jude, A. L. Banerjee, M. Haldar, S. Manokaran, J. Kooren, S. Mallik, D. W. Christianson, "Structural analysis of charge discrimination in the binding of inhibitors to human carbonic anhydrases i and ii," J. Am. Chem. Soc. 129 (17) (2007) 5528–5537.

[24] M. B. Peters, Y. Yang, B. Wang, L. Füsti-Molnár, M. N. Weaver, K. M. Merz, "Structural Survey of Zinc-Containing Proteins and Development of the Zinc AMBER Force Field (ZAFF)," Journal of Chemical Theory and Computation 6 (9) (2010) 2935–2947. doi:10.1021/ct1002626.

[25] C. Liu, B. Zhang, Y. Zhu, M. Tang, "Evaluations of AMBER force field parameters by MINA approach for copper-based nucleases," Struct. Chem. 27 (5) (2016) 1449–1464.

[26] Y. Zhu, Y. Su, X. Li, Y. Wang, G. Chen, "Evaluation of Amber force field parameters for copper(II) with pyridylmethyl-amine and benzimidazolylmethyl-amine ligands: A quantum chemical study," Chem. Phys. Lett. 455 (4-6) (2008) 354–360.

[27] M. J. Frisch, G. W. Trucks, H. B. Schlegel, G. E. Scuseria, M. A. Robb, J. R. Cheeseman, G. Scalmani, V. Barone, B. Mennucci, G. A. Petersson, H. Nakatsuji, M. Caricato, X. Li, H. P. Hratchian, A. F. Izmaylov, J. Bloino, G. Zheng, J. L. Sonnenberg, M. Hada, M. Ehara, K. Toyota, R. Fukuda, J. Hasegawa, M. Ishida, T. Nakajima, Y. Honda, O. Kitao, H. Nakai, T. Vreven, J. A. Montgomery, Jr., J. E. Peralta, F. Ogliaro, M. Bearpark, J. J. Heyd, E. Brothers, K. N. Kudin, V. N. Staroverov, R. Kobayashi, J. Normand, K. Raghavachari, A. Rendell, J. C. Burant, S. S. Iyengar, J. Tomasi, M. Cossi, N. Rega, J. M. Millam, M. Klene, J. E. Knox, J. B. Cross, V. Bakken, C. Adamo, J. Jaramillo, R. Gomperts, R. E. Stratmann, O. Yazyev, A. J. Austin, R. Cammi, C. Pomelli, J. W. Ochterski, R. L. Martin, K. Morokuma, V. G. Zakrzewski, G. A. Voth, P. Salvador, J. J. Dannenberg, S. Dapprich, A. D. Daniels, O. Farkas, J. B. Foresman, J. V. Ortiz, J. Cioslowski, D. J. Fox, "Gaussian 09, Revision E.01."

[28] P. Li, K. M. Merz, "Mcpb.py: A python based metal center parameter builder," Journal of Chemical Information and Modeling 56 (4) (2016) 599–604.

[29] W. L. Jorgensen, J. Chandrasekhar, J. D. Madura, R. W. Impey, M. L. Klein, "Comparison of simple potential functions for simulating liquid water," J. Chem. Phys. 79 (2) (1983) 926–935.

[30] R. Salomon-Ferrer, D. A. Case, R. C. Walker, "An overview of the amber biomolecular simulation package," WIREs. Comput. Mol. Sci. 3 (2) (2013) 198–210.

[31] D. R. Roe, T. E. Cheatham, "Ptraj and cpptraj: Software for processing and analysis of molecular dynamics trajectory data," J. Chem. Theory Comput. 9 (7) (2013) 3084–3095.

[32] M. Zacharias, T. P. Straatsma, J. A. McCammon, F. A. Quiocho, "Inversion of Receptor Binding Preferences by Mutagenesis: Free Energy Thermodynamic Integration Studies on Sugar Binding to l-Arabinose Binding Proteins," Biochemistry 32 (29) (1993) 7428–7434.

[33] Y. Andoh, K. Oono, S. Okazaki, I. Hatta, "A molecular dynamics study of the lateral free energy profile of a pair of cholesterol molecules as a function of their distance in phospholipid bilayers," J. Chem. Phys. (2012) 155104.

[34] K. Fujimoto, N. Yoshii, S. Okazaki, "Free energy profiles for penetration of methane and water molecules into spherical sodium dodecyl sulfate micelles obtained using the thermodynamic integration method combined with molecular dynamics calculations," J. Chem. Phys. (2012) 094902.

[35] S. Kawada, K. Fujimoto, N. Yoshii, S. Okazaki, "Molecular dynamics study of the potential of mean force of SDS aggregates," J. Chem. Phys. (2017) 084903.

[36] K. Kawaguchi, S. Nakagawa, I. Kurniawan, K. Kodama, M. S. Arwansyah, H. Nagao, "A coarse-grained model of the effective interaction for charged amino acid residues and its application to formation of gcn4-pli tetramer," Mol. Phys. 116 (5-6) (2018) 649–657.

[37] T. Shuku, K. Sugimori, A. Sugiyama, H. Nagao, T. Sakurai, K. Nishikawa, "Molecular orbital analysis of active site of oxidized azurin: Dependency of electronic properties on molecular structure," Polyhedron 24 (16-17) (2005) 2665–2670.

[38] I. Kurniawan, T. Matsui, K. Kawaguchi, H. Nagao, "Theoretical studies on association/dissociation process of plastocyanin and cytochrome f in photosynthesis," J. Phys.: Conf. Ser. (in press).

[39] A. Casini, J. Y. Winum, J. L. Montero, A. Scozzafava, C. T. Supuran, "Carbonic anhydrase inhibitors: Inhibition of cytosolic isozymes I and II with sulfamide derivatives," Bioorganic and Medicinal Chemistry Letters 13 (5) (2003) 837–840.

[40] V. Alterio, S. M. Monti, E. Truppo, C. Pedone, C. T. Supuran, G. De Simone, "The first example of a significant active site conformational rearrangement in a carbonic anhydrase-inhibitor adduct: the carbonic anhydrase i-topiramate complex," Org. Biomol. Chem. 8 (2010) 3528–3533.

[41] A. Zubrienė, J. Smirnovienė, A. Smirnov, V. Morkūnaitė, V. Michailovienė, J. Jachno, V. Juozapaitienė, P. Norvaišas, E. Manakova, S. Gražulis, D. Matulis, "Intrinsic thermodynamics of 4-substituted-2,3,5,6-tetrafluorobenzenesulfonamide binding to carbonic anhydrases by isothermal titration calorimetry," Biophysical Chemistry 205 (2015) 51–65. doi:https://doi.org/10.1016/j.bpc.2015.05.009.

[42] N. Chiaramonte, M. Romanelli, E. Teodori, C. Supuran, "Amino Acids as Building Blocks for Carbonic Anhydrase Inhibitors," Metabolites 8 (2) (2018) 36.

[43] M. K. Gilson, J. A. Given, B. L. Bush, J. A. McCammon, "The statistical-thermodynamic basis for computation of binding affinities: A critical review," Biophysical Journal 72 (3) (1997) 1047–1069.

[44] S. K. Choubey, D. Prabhu, M. Nachiappan, J. Biswal, J. Jeyakanthan, "Molecular modeling, dynamics studies and density functional theory approaches to identify potential inhibitors of sirt4 protein from homo sapiens : a novel target for the treatment of type 2 diabetes," Journal of Biomolecular Structure and Dynamics 35 (15) (2017) 3316–3329.

[45] K. A. Brown, Y. Zou, D. Shirvanyants, J. Zhang, S. Samanta, P. K. Mantravadi, N. V. Dokholyan, A. Deiters, "Light-cleavable rapamycin dimer as an optical trigger for protein dimerization," Chem. Commun. 51 (2015) 5702–5705.

[46] B. R. Miller, T. D. Mcgee, J. M. Swails, N. Homeyer, H. Gohlke, A. E. Roitberg, "MMPBSA . py : An Efficient Program for End-State Free Energy Calculations," J. Chem. Theory Comput. 8 (9) (2012) 3314–3321.